Check for updates

Assessment of water resources system resilience under hazardous events using system dynamic approach and artificial neural networks

Milan Stojković [a],*, Dusan Marjanović[b], Dragan Rakić[c], Damjan Ivetić[d], Višnja Simić[e], Nikola Milivojević[a] and Slaviša Trajković[f]

[a] Institute for Artificial Intelligence R&D Serbia, Novi Sad, Serbia
[b] Jaroslav Černi Water Institute, Belgrade, Serbia
[c] Faculty of Engineering, University of Kragujevac, Kragujevac, Serbia
[d] Faculty of Civil Engineering, University of Belgrade, Belgrade, Serbia
[e] Faculty of Science, University of Kragujevac, Kragujevac, Serbia
[f] Faculty of Civil Engineering and Architecture, University of Niš, Niš, Serbia
*Corresponding author. E-mail: milan.stojkovic@ivi.ac.rs

MS, 0000-0002-7817-9341

ABSTRACT

The objective of this research is to propose a novel framework for assessing the consequences of hazardous events on a water resources system using dynamic resilience. Two types of hazardous events were considered: a severe flood event and an earthquake. Given that one or both hazards have occurred and considering the intensity of those events, the main characteristics of flood dynamic resilience were evaluated. The framework utilizes an artificial neural network (ANN) to estimate dynamic resilience. The ANN was trained using a large, generated dataset that included a wide range of situations, from relatively mild hazards to severe ones. A case study was performed on the Pirot water system (Serbia). Dynamic resilience was derived from the developed system dynamics model alongside the hazardous models implemented. The most extreme hazard combination results in the robustness of 0.04, indicating a combination of an earthquake with a significant magnitude and a flood hydrograph with a low frequency of occurrence. In the case of moderate hazards, the system robustness has a median value of 0.2 and a rapidity median value of 162 h. The ANN's efficacy was quantified using the average relative error metric which equals 2.14% and 1.77% for robustness and rapidity, respectively.

Key words: flood dynamic resilience, flood risk assessment, machine learning, Pirot water resources system, system dynamics modeling approach

HIGHLIGHTS

- Proposition of a generalized methodological framework to quantify flood dynamic resilience of water systems using a significant amount of generated data related to multiple hazards.
- Implementation of the results derived from the dam safety model for accurate estimation of the earthquakes' impacts.
- Application of ANN to predict the main characteristics of the flood-risk related matrices.

Assessment of Water Resources System Resilience Under Hazardous Events Using System Dynamic Approach and Artificial Neural Networks
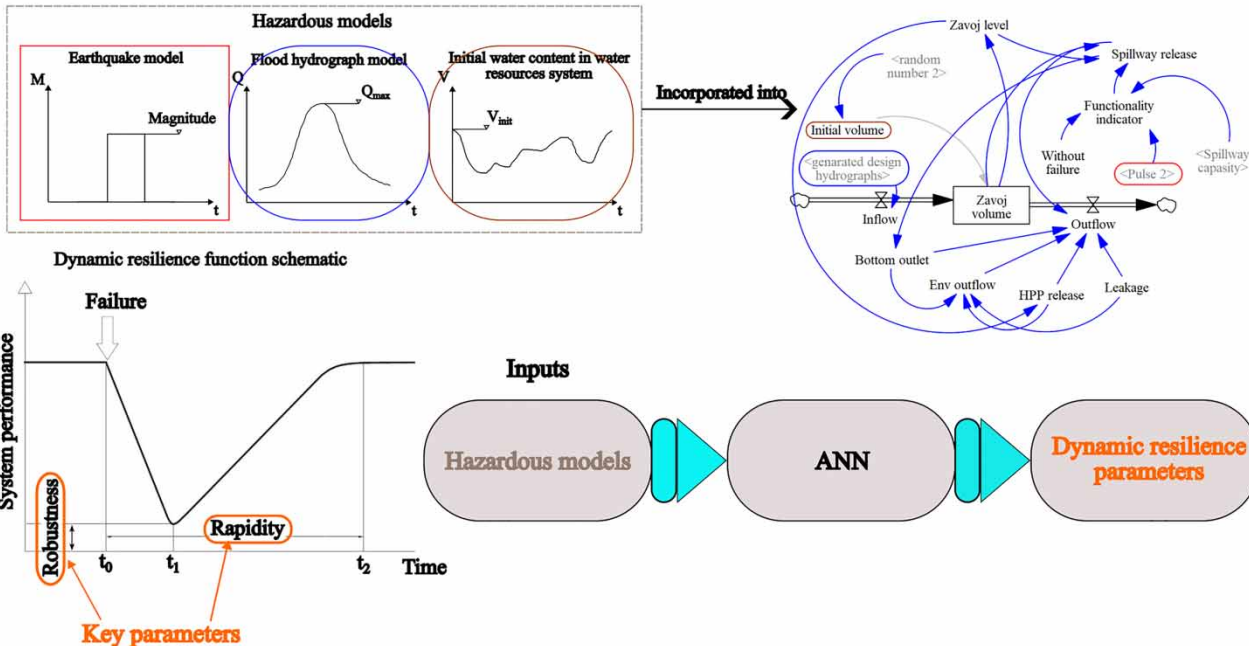
INTRODUCTION

Water resources systems are designed to withstand demands imposed by their service requirements (Simonovic 2021). However, their flood protection facilities are designed by existing standards and under the present climate. Considering the aging process and rapid changes in the environment (e.g., climate variability, climate change, natural hazards), they do not necessarily guarantee an adequate level of service and safety. Hence, major investment is required to renew and upgrade these aging water systems to adapt to the rapidly growing population, whose future is affected by changing climate and natural disasters (e.g., floods, earthquakes).

Climate change leads to flood events characterized by greater frequency and more severity (Liang *et al.* 2019), and therefore greatly impacts the probabilistic behavior of extreme annual streamflows (Xu *et al.* 2020). Given that, one of the main roles of water systems is responding to natural disasters, such as floods, by controlling the outflow from the water system (Men *et al.* 2019; Yang *et al.* 2022). To cope with such hazards under present and future climate, water resources systems have to be revitalized for several reasons, such as poor initial design of the water system, rapid changes in the downstream river sections (e.g., urbanization), and safety requirements by increasingly risk-averse societies (Bocchiola & Rosso 2014).

Alongside climate-related risks, earthquakes also present a significant hazard that can reduce the safety of the water resources system (ICOLD 2018). Earthquakes commonly trigger landslides producing consequences ranging from small soil cover failures to devastating rock avalanches (Fan *et al.* 2019). As a part of a water system, a large dam can fail under severe seismic conditions leading to uncontrolled release from the system, and require optimal operational rules for gated spillways (Haktanir *et al.* 2013). Moreover, a water resources system located within a high seismic area possesses a substantial risk for the downstream river sections since active faults may cause damaging deformation of the embankment leading to uncontrolled water system behavior (Tosun 2015).

Risk analysis of the water resource systems needs to consider a variety of hazardous events (e.g., floods, earthquakes), or a combination of events that could lead to the failure of the system (Bowles *et al.* 2013). It can be performed through the qualitative or quantitative description of potential hazardous scenarios including external threats (e.g., earthquakes, floods),

internal threats (e.g., failure of the system elements), dam failures, etc. The identification of potentially hazardous events is commonly quantified using expert opinions regarding the occurrence probability of hazards, their severity as well as detectability (Ardeshirtanha & Sharafati 2020). Generally, the four-step procedure shown in Table 1 is usually applied to identify core hazardous scenarios leading to loss of strength and water tightness, or even a breach of the dam (Bowles *et al.* 2013).

As an essential treatment of the water resources system functionality, a procedure for the identification of potentially hazardous events highlights a combination of hazards that can jeopardize the water system services and safety. In contrast to a single hazard risk assessment, quantification of multiple hazards represents a challenging issue within risk analysis, including hazard assessment, vulnerability characterization, and risk assessment (De Angeli *et al.* 2022). Multiple hazards arise from the spatial and temporal coincidence of potentially interconnected hazards affecting the water system elements and level of safety (Kappes *et al.* 2012). Their relationships primarily consider a situation where the first hazard triggers or increases the probability of secondary hazards occurring (Gill & Malamud 2014). This can be achieved by using visualization techniques based on the large amounts of the recorded hazards (Kappes *et al.* 2012).

Furthermore, a multi-hazard modeling approach can be implemented within the mathematical framework, consisting of risk analysis, analytic hierarchy processing, and fuzzy logic to examine multi-hazard interactions and to provide a comprehensive risk assessment of the water resources systems (Jiang & Zhang 2008; Greco *et al.* 2012; Hwang *et al.* 2015; Assumma *et al.* 2019; Nozari *et al.* 2021; Datola *et al.* 2022; De Angeli *et al.* 2022). A general framework for multi-hazard modeling is based on the use of component operating states database of the water resources system, where the failure scenarios are simulated via the application of the deterministic Monte-Carlo (MC) approach to determine a wide range of water system behaviors for each scenario (King & Simonovic 2020). The generated scenarios vary the timing and severity of hazardous events as well as the inflows in the water resources system capturing the system's response to the full range of potential operating conditions (King *et al.* 2019).

However, the flood risk assessment frameworks do not research in detail the coincidence of hazardous events with low joint frequencies and their impacts on the water system behavior, mainly because a wide range of potential hazardous events and the system's responses require machine learning techniques to deduce the knowledge from a significant amount of data. Additionally, the system response to hazards, like earthquakes, imposes the use of a numerical dam safety model to precisely extract the relationship between the system element functionality and earthquake magnitude (Rakić *et al.* 2022). To examine the impacts of natural hazards with a high magnitude and low joint frequencies on the water resources system functionality, the presented research proposes the usage of a system dynamics modeling approach underpinned by artificial neural networks (ANNs) for flood-related risk prediction. It incorporates the developed water resources system and hazardous models, as well as outputs from the dam safety model. The outputs from system dynamics models are used for flood dynamic resilience evaluation since it is selected as a time-dependent flood risk metric (Ignjatović *et al.* 2021). Implemented within the system dynamics modeling approach, hazardous events include the spatial and temporal coincidence of flood and earthquake under stochastically generated inputs, followed by the variable initial state in the water resources system. An ANN is then trained over the generated inputs and outputs from the system response to quantify the flood-related risks in real-time and to support the decision-making process within the river basin under hazardous events.

Therefore, the goals of the presented research are given as follows: (1) proposition of a generalized methodological framework to quantify flood dynamic resilience of water system using a significant amount of generated data related to multiple

Table 1 | Identification of hazardous events of the water resources system: a four-step procedure

Step 1	Step 2	Step 3	Step 4
Description of water system elements, their mutual interdependence, and their roles in preventing water systems failures (Bowles *et al.* 2013).	Identify potential hazardous events leading to the failure of a water system. Providing a list of significant external hazards with the potential to initiate water system failure (Bowles *et al.* 2013).	Consider the potential sets of hazards, as a substantial and physically possible failure event, alongside their impacts on the system functionality, that can lead to the water system failure (Environment Agency 2011; Bowles *et al.* 2013).	Segregate hazardous events in terms of water system functionality as significant or not significant. Choose the most realistic significant combinations of hazards to estimate the water system risk (Bowles *et al.* 2013).

hazards (e.g. floods, earthquakes, variable state of the system), (2) implementation of the results derived from the dam safety model for accurate estimation of the earthquakes' impacts on the water resources system functionality, and (3) application of ANN to predict the main characteristics of the flood-risk related matrices (flood dynamic resilience) based on the water system response.

The paper is structured in the following way: the first section envelopes the methodological approaches for developing the system dynamic model, hazardous models, and dynamic resilience assessment of the water resource system. Next, the case study illustrates the selected water resource system located in Serbia (southeast Europe). Afterwards, the results of the proposed methodology are depicted to illustrate model development and simulations performed. The next section discusses the results and links them to relevant research from the literature. In the final section, the implications of the presented research are discussed and directions for future research are proposed.

METHODS

General approach

The main objective of this research is to devise a generalized risk-based methodology for the evaluation of flood dynamic resilience of water resources systems using machine learning. To achieve this objective, a system dynamics (SD) model is developed to mimic the non-linear behavior of the water resource system. It provides information required for flood dynamic resilience assessment as a wide range of possible outcomes depending on the initial reservoir levels, inflows, and timing of events (King & Simonovic 2020). The SD model is supported by hazardous models which introduce the time coincidence of several unexpected hazardous events (earthquakes, floods, and changeable water content in a reservoir). Specifically, the earthquake hazardous model simulates the impact of earthquakes on the element of the system reservoir (e.g., the impact of the decreased capacity of the gated spillway). A flood dynamic over the simulation period is represented by the flood hydrograph model, as a part of hazardous modeling. Moreover, the changeable initial water content in the reservoir at the time of system failure is generated since the gate's operation depends on inflows and the initial state in a system. The hazardous models introduce the randomized model parameters enabling the generation of hazardous events with different magnitudes, especially in terms of low-frequency hazardous events. Alongside the SD model, hazardous models support the assessment of flood dynamic resilience for a variety of possible scenarios. Then, a number of the generated hazardous events and estimated dynamic resilience are used as a solid basis for the extraction of the knowledge from the generated data via ANN. The ANN captures the important characteristics of dynamic resilience and enables its application for real-time decision-making in a water resources system.

The proposed ANN framework for the evaluation of dynamic resilience of water resources systems under hazardous events is illustrated in Figure 1. Individual parts of a general flood risk assessment framework are described in more detail further in the paper.

Hazardous models

Flood hydrograph model

A deterministic, distributed-parameter, physical process-based hydrologic model (Precipitation-Runoff Modeling System) is used to generate the long-term flow sequences (Ignjatović et al. 2021). It enables the evaluation of the hydrological response based on various climate combinations including the generated long-term sequences of climate data. As the inputs for the hydrological model, the stochastically generated climate data by weather generator is utilized (Ignjatović et al. 2021). The non-parametric K-nearest neighbor (K-NN) weather generator is employed by reshuffling the recorded value of precipitation as well as minimal and maximal air temperature as a basis for daily streamflow assessment (King et al. 2015). Additionally, the reshuffled climate records are perturbed with the aim of generating climate data beyond the historically observed values. Such generated data are used to force a hydrological model to produce daily streamflows over long-term periods.

In this study, the annual maximum series approach is applied to estimate low flood frequencies from the generated annual streamflows (Karim et al. 2017). The general extreme value (GEV) distribution is fitted to annual maximum streamflows since it provides the best fit for extreme flow as well as precipitation data within the region analyzed (Stojković et al. 2017; Gocić et al. 2021). By application to the hydrological data, the flood magnitudes with different return periods (T) are estimated. In addition, the shape of a theoretical flood hydrograph is approximated by the Gumbel distribution (Manfreda et al. 2021). Using the flood magnitude and shape of the flood hydrograph, flood hydrographs $Q(t)$ are defined for the set of return periods.
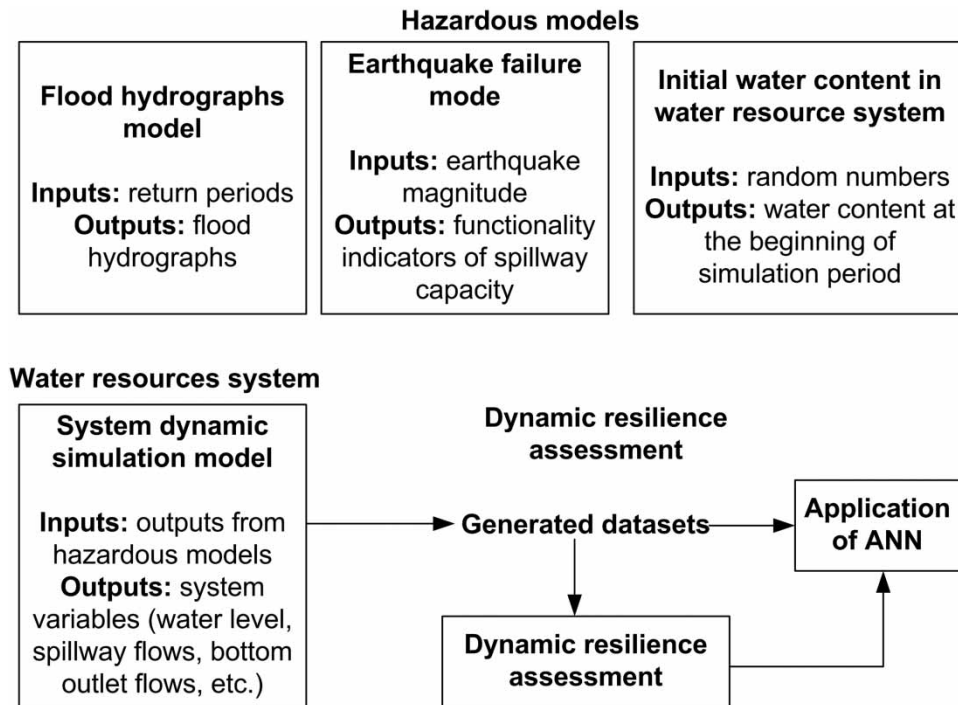
Figure 1 | A general approach for evaluation of flood dynamic resilience for the water resources system under hazardous events.

Next, flood hydrographs are generated using MC simulations founded upon uniform distribution defined as lower and upper bounds:

$$Q = \text{MCS} \left\{ \begin{array}{l} \text{Lower bound} = T_{100 \text{ years}} \\ \text{Upper bound} = T_{10,000 \text{ years}} \end{array} \right\} \tag{1}$$

Earthquake model

The varying earthquake events are generated as a stress test of the water resources system addressing the adverse impacts on the water resources system elements considering the fact that earthquakes have frequently occurred within the analyzed area and wider (Maršanić *et al.* 2021).

A numerical analysis of the water resources system elements is performed using the finite element method (Rakić *et al.* 2022). The result of the numerical analysis identifies key structural elements with potential influence on water system performance. For the purpose of this study, a simplified analytical form of the effective spillway capacity (ESWC) of the water resources system is utilized (Rakić *et al.* 2022):

$$\text{ESWC} = 1 + 0.0529a + 0.0843a^2 - 0.7087a^3 \tag{2}$$

where a represents the standardized magnitude of earthquake simulated by MC simulation in the range from 0 to 1.

Hence, the earthquake model is explicitly used in this dependence resulting in a functionality indicator of the system element to describe a physical drop of the ESWC and corresponding effects in the system operation (Ignjatović *et al.* 2021). The functionality indicator (α) depending on simulation time $t \in [t_{\text{start}}, t_{\text{end}}]$ also incorporates the earthquake start time (t_0) and recovery time (t_1) needed to retrieve the full system element performance:

$$\alpha = \left\{ \begin{array}{ll} 1, & \text{for } t < t_0 \\ 0 < \text{ESWC} < 1, & \text{for } t \in [t_0, t_1] \\ 0, & \text{for } t > t_1 \end{array} \right\} \tag{3}$$

where the start time (t_0) coincides with the flood hygrograph occurrence (Gill & Malamud 2014). On the contrary, recovery time (t_1) strictly depends on the earthquake magnitude.

Initial water state model

The modeling of the water resources system involves an initial water state (V_{start}) in the reservoir at the first stage of decision making at t_{start} (Kistenmacher & Georgakakos 2015). The state in the reservoir at the next simulation stage ($V_{\text{start}+1}$) is estimated by applying the first stage decisions (e.g., gates opening and hydropower release at t_{start}) and first stage inflow (Q_{start} at t_{start}).

Fluctuations of the water state in the system, expectedly, range from the states at minimal operation level to the corresponding state at maximal operation level. It is more likely that stage decisions keep the water level in the reservoir around the normal water level which enables the water resource system to mitigate and attenuate flood hydrograph.

Therefore, an initial state (V_{start}) in the water resources system is simulated using the triangular distribution as an input for MC simulations (Major 2019). The triangular distribution is a continuous three parameter distribution with the most likely distribution value limited by extreme values, particularly with lower and upper bounds. Following this, the initial water states are simulated using the aforementioned parameters and referent operational levels (minimal, normal, and maximal):

$$V_{\text{start}} = \text{MCS} \begin{cases} \text{Lower bound} = \text{water state at minimal operational level} \\ \text{Most likely value} = \text{water state at normal operational level} \\ \text{Upper bound} = \text{water state at maximal operational level} \end{cases} \tag{4}$$

Water resources system model

The SD simulation model with a causal loop is developed to mimic the behavior of the water resources system. It is characterized by the following blocks (Ahmad & Simonovic 2000; Stojkovic & Simonovic 2019; Ignjatović et al. 2021): stocks, flows, and connectors. Stocks represent the level of variable balancing among flows, for instance, the inflows and outflows from the water resources system. Variables are used to analytically define the functions needed for system reservoir operations connectors, while connectors direct the variables, inflows, and levels enabling the SD model for real operational usage.

The SD model incorporates causal loops providing a link between the system characteristics, inputs, and operational rules separately defined for flood protection facilities (spillway and bottom outflow) and hydropower plants (Stojkovic & Simonovic 2019). System characteristic describes the main parameters of the water system such as water storage curve, spillway, bottom outflow hydraulic characteristics, and hydropower plant parameters. The SD model incorporates an additional model structure defined as functional indicators since they implicitly describe the reduced capacity of the water system elements caused by natural or man-made hazardous events (Ignjatović et al. 2021).

The SD model is developed in this research to mimic a multipurpose water resources system highlighting the flood management reservoir roles. It releases outflows from the spillway (Q_{SW}) and the bottom outflow facility (Q_{BO}). Additional water management roles are also incorporated within the SD model allowing for the control of the discharge to suit the demand for hydropower generation (Q_{HPP}) and ecological flow improvements during low-flow periods (Q_{ENV}). In addition, the losses from the water resources system are taken into account as leakage from the dam (Q_{L}).

The inputs in the SD models are the initial water state, flood hydrographs $Q(t)$, total releases from water systems (Q_{SW}, Q_{BO}, Q_{HPP}, Q_{ENV}), functionality indicator of the spillway (α), and losses (Q_{L}). Considering the input for the SD model, its output is defined as the water state (V) in the system over simulation time t (Stojkovic & Simonovic 2019):

$$V(t) = V_{\text{start}} + \int_{t_{\text{start}}}^{t_{\text{end}}} [Q(t) - (\alpha(t) \cdot Q(t)_{\text{SW}} + Q(t)_{\text{BO}} + Q(t)_{\text{HPP}} + Q(t)_{\text{ENV}} + Q(t)_{\text{L}})]dt \tag{5}$$

Dynamic resilience assessment

Over a disruptive event that poses a serious threat to the water resources system and belonging elements, a dynamic resilience model captures several numerical characteristics. The most important of these are robustness and rapidity, illustrated in Figure 2. Robustness represents the ability of the system to resist disturbance, while rapidity is the capacity to return the system to a predisturbance level of functioning (Simonovic & Arunkumar 2016). Once the water system does not provide the required services under an unexpected hazardous event, dynamic resilience starts to decrease to the lowest resilience
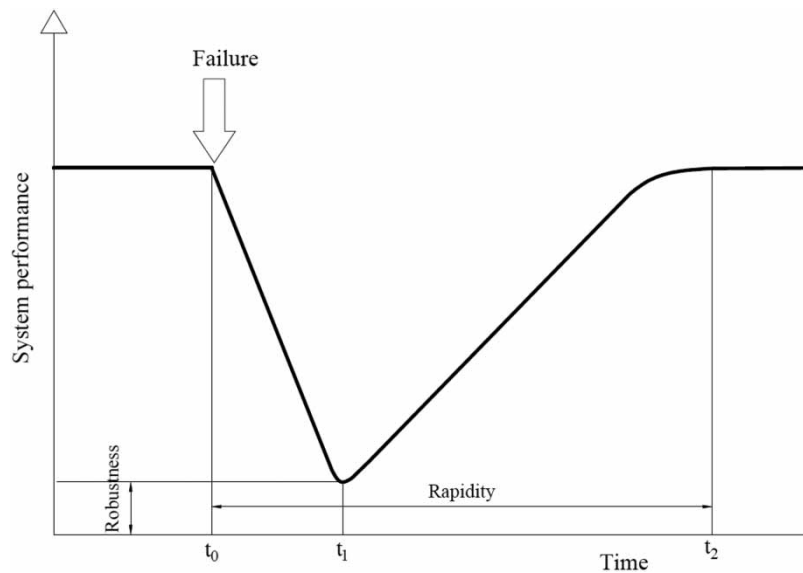
Figure 2 | Schematic representation of the dynamic resilience function: robustness and rapidity.

level expressed as robustness (Figure 2). Then, the adaptive capacity of a system called rapidity leads to increasing a system's resilience at the highest possible level.

A simulated earthquake coinciding with high-flow river conditions and variable initial state in the water resources system influences the system elements by reducing the system's capacity to respond and withstand during the hazardous event. The loss of reservoir capacity is defined as the loss of the volume in the water system needed to receive the flood hydrograph. On the contrary, the degree of flood peak attenuation is the reservoir's capacity to respond to the flood event.

The loss of water resources system capacity leads to a decrease in flood dynamic resilience because the system cannot provide the designated system services. Therefore, the flood dynamic resilience (r) depicted in Figure 2 is defined in an analytical form (Simonovic & Arunkumar 2016):

$$r(t) = 1 - \left(\frac{P_0(t - t_0) - \sum_{t_0}^{t} P(t)}{P_0(t - t_0)} \right) \tag{6}$$

where P denotes the system performance level at the current time step t, while P_0 describes the initial system performance level at the time of the hazardous event t_0.

In our study, the system performance level respects the current water level in the water system alongside referent water levels for flood management operation:

$$P = \left\{ \begin{array}{ll} 1, & \text{water level } \leq \text{maximal operational level} \\ 0, & \text{water level } > \text{maximal operational level} \end{array} \right\} \tag{7}$$

Flood dynamic resilience represents a time-dependent risk metric (Equation (7)) controlled by the capacity of the spillway to evacuate an excess water volume from the water system maintaining the system below acceptable water levels, for instance, maximal operational level. However, the transformation of flood hydrographs within the system is demanded since it coincides with a reduced capacity of the spillway gates caused by the earthquake. Moreover, the variable initial water state can increase the flood-related risk as the initial water level exceeds the expected water level in the reservoir.

Taking into account the fact that the flood dynamic reliance depends on hazards with variable magnitude, time of occurrence, and duration, there is a need to generalize the assessment of dynamic resilience using an ANN. Application of the

ANN provides information on the dynamic resilience in a timely manner and enables the prediction needed to perform adequate strategies aimed at reducing the adverse effect on the environment caused by external hazardous inputs. The previously developed ANN algorithm (Beale *et al.* 2020) is adopted to extract the information from the flood dynamic resilience of the system (Equation (7)) expressed as the robustness and rapidity, using randomly generated hazardous events with different impacts on the system elements (Equations (1), (3), and (4)).

For each simulation, the SD model generates a random hazardous model and, in a general sense, a functional dependence in the ANN model can be written as:

$$(\text{Robustness, Rapidity}) = f[Q_{max}, \alpha_{min}, V_{start}] \tag{8}$$

where Q_{max} is a peak of the simulated flood hydrograph (Equation (1)), α_{min} represents a total reduction of spillway capacity representing a functionality indicator of the spillway (Equation (3)), and V_{start} is the volume in the water resources system at the moment of failure (Equation (4)), thus a function in Equation (8) is formed from the SD model inputs and outputs. A feedforward ANN is trained using Levenberg–Marquardt (LM) learning algorithm and sigmoid activation function to model the function presented in Equation (8) (Beale *et al.* 2020).

CASE STUDY

The Pirot water resources system is located in southeast Serbia (Figure 3(a)) extending over a flood-prone area (the upper basin of the Nišava river) of around 571 km². It represents a complex water resources system including the Zavoj reservoir at the Visočica river, hydraulically connected by a pressure tunnel with the hydropower plant (HPP) Pirot. The HPP Pirot conveys the HPP outflows from the Visočica river to the Nišava river. The scheme of the Pirot water system is given in Figure 3(b).

The primary purpose of the Pirot water system is the mitigation of floods at the Nišava river, hydropower generation, and downstream water quality control by regulation of the outflows from the reservoir over the low-flow seasons. The management of the Pirot water system depends on the actual volume of water stored in the reservoirs, inflows, and energy demand (Ignjatović *et al.* 2021). The active storage of the Zavoj reservoir is 140×10^6 m³ (Table 2). Three gated spillways are located at the left part of the dam with a capacity of 1,820 m³/s. The power plant has two turbines (40 MW) for power generation, with an installed capacity of 45 m³/s (Table 2). The Zavoj reservoir is hydraulically connected with diversion-type turbines at the HPP Pirot by the 9 km pressure tunnel with a 4.5 m radius. The pressure tunnel conveys the water from the Visočica river to the Nišava river providing a significant contribution to the total annual flow of the downstream river.
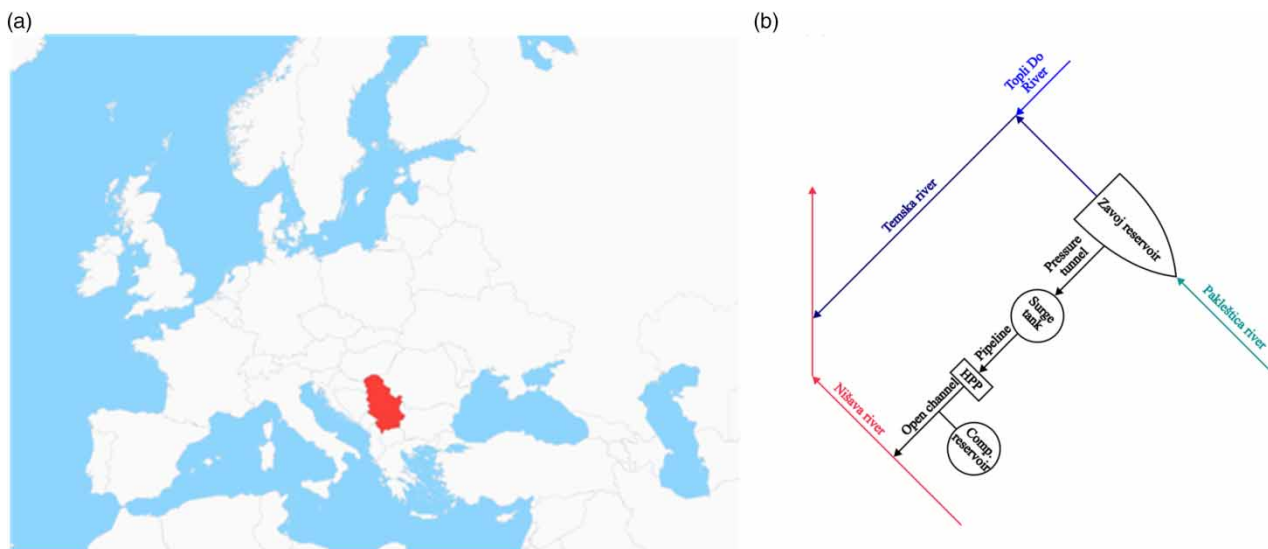

Figure 3 | Location of Serbia at the European regional scale (a) and schematic representation of the Pirot water system (b).

Table 2 | The characteristics of the Zavoj reservoir in the Pirot water resources system

Reservoir	Year built	Drainage area (km²)	Annual inflows (m³/s)	Active volume (10⁶ m³)	Flood storage volume (10⁶ m³)	Minimal operational level (m a.s.l.)	Spillway capacity (m³/s)
Zavoj	1990	571	6.2	140	5.5	568	1,820

RESULTS

Hazardous models

The variability of flood events was simulated by applying a random selection of return periods. Next, the generated earthquake magnitudes were introduced as additional pressure on the system functionalities by reducing the spillway capacity. Depending on the earthquake magnitudes, the decreased capacity of the spillway was simulated by employing the empirical law (Equation (2)). Moreover, a variable initial state (volume) in the Zavoj reservoir was also randomly generated respecting the physical limitations of the reservoir (referent operation levels).

Flood hydrograph model

The deterministic hydrological model provided the long-term daily flows for a 1,000-year time frame at the site of the Zavoj reservoir. For the sake of the hydrological simulations, the generated precipitation and air temperature from the K-NN water generator were used. The annual maximum series approach had chosen the most extreme annual flows, and then the GEV distribution was applied to estimate the design annual flows with different return periods (from 100- to 10,000-year return periods). To define the flood hydrographs, the Gumbel distribution was used to shape the flood hydrographs and respect the design of annual flows.

The empirical and theoretical (GEV) cumulative distributions of the maximal annual flows at the Zavoj reservoir are depicted in Figure 4(a), while the flood hydrographs for different return periods are provided in Figure 4(b). As can be seen from Figure 4, a flood hydrograph with a 10,000-year return period exceeds the total capacity of the spillway (Table 3), while the lower flood frequencies (from 100- to 1,000-year return periods) remain below the maximal spillway capacity.

Once the flood hydrographs had been estimated, a generation of flood hydrographs was performed via the MC simulations as the input for the SD model simulations. For the purpose of hydrograph generation, a uniform distribution was applied to form a dataset of 1,000 members (Table 3).
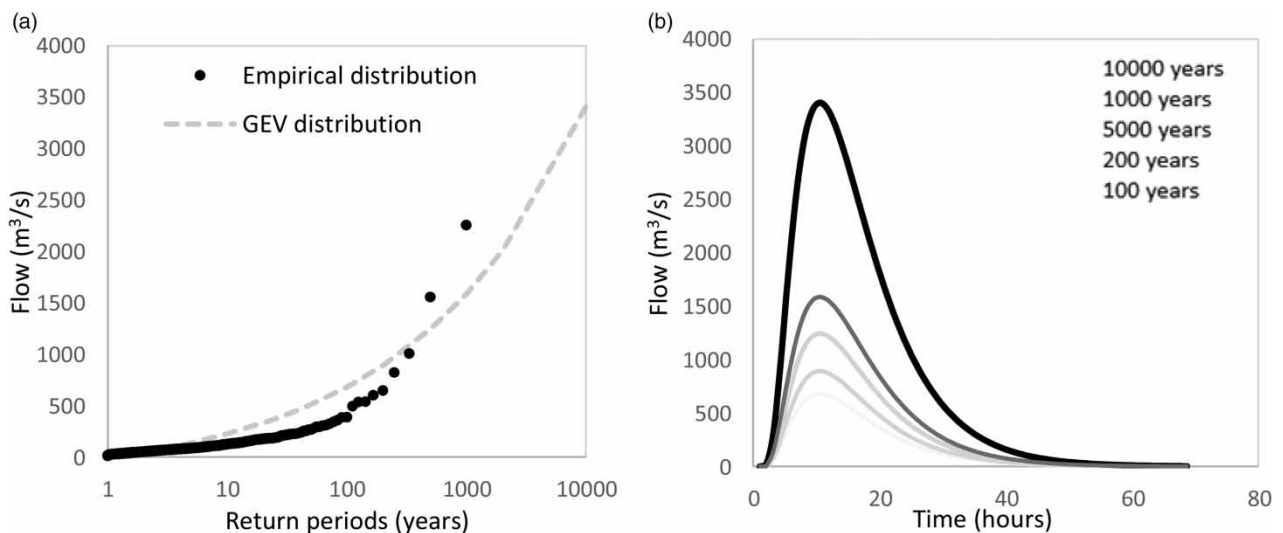

Figure 4 | Annual maximum flows (a) and flood hydrographs for different return periods (b) at the Zavoj reservoir (Pirot water resources system).

Table 3 | Used distribution and its parameters within the hazardous models of the Pirot water resources system

Hazardous models	Distribution type	Distribution parameters
Flood hydrograph model – Return period (T)	Uniform distribution	(10,0000–100 years)
Earthquake hazardous model – Standardized magnitude of the earthquake (a)	Uniform distribution	(0,1)
Initial water state model (V_{start})	Triangular distribution	($1.3362 \times 10^{+08}$ m^3, $1.572 \times 10^{+08}$ m^3, $1.8078 \times 10^{+08}$ m^3)

Earthquake model

The impact analysis of the earthquake magnitudes on the spillway capacity reduction was carried out considering the range of possible seismic acceleration within the analyzed region (Rakić *et al.* 2022). Given that, the dependence between the spillway capacity and earthquake magnitude was deduced from the numerical stability model of the Zavoj dam resulting in empirical values of ESWC (Equation (2)).

To generate the dataset of 1,000 values, the MC approach (Table 3) was performed using a uniform distribution of the standardized magnitude of the earthquake (a). Furthermore, the spatial and temporal coincidence of natural hazards within the upper Nišava river basin was taken into account with respect to flood hydrograph occurrence. Having obtained the ESWC values, start time (t_0) and recovery time (t_1), the functionality indicators of the spillway were determined for each generated earthquake following Equation (3).

Initial state model

Initialization of the SD model of the Pirot water resources system was performed using the same number of MC simulations. Namely, each simulation has a statically generated initial water state in the Zavoj reservoir varying between maximal and minimal operational levels (Table 3). Moreover, the most probable initial state in the reservoir corresponds to the normal operating level. For these reasons, the simulation was performed following the triangular distribution whose median matches the normal operational level, while the distribution is limited by two extreme operational levels (maximal and minimal).

Water resources system model

System dynamics simulation was used to model interactions between the water resources system inputs, system elements, and outputs. In this research, the SD model of the multipurpose Pirot water resources system represents the following system elements: spillway and bottom outflow facilities, hydropower plant, and leakage from the Zavoj Dam. Spillway (Q_{SW}) and bottom outflow releases (Q_{BO}) serve to control and reduce the devastating impact of the flood events at the downstream river sections of the Visočica and Nišava rivers. Moreover, bottom outflow releases improve the water quality of the Visočica river during the low-water periods, usually during the summer and autumn months. Depending on the energy market's demands, the operator of the Pirot water system controls the hydropower generation releases (Q_{HPP}) considering the physical and environmental limitations to supply the energy market over peak demand hours.

The SD model of the Pirot water resources system was implemented on an hourly basis, within the system dynamics software (Vensim Reference Manual 2021; VenPy 2022), to provide an adequate system response to dynamical hazardous events (e.g., rapid flood genesis). The differential equation of the water resources system (Equation (5)) was solved by the Euler integration method. This explicit integration method takes into account the state of the system at a later time ($t - 1$) to calculate the state at the current simulation time (t). A schematic representation of the SD model of the Pirot water resources system is depicted in Figure 5(a) together with the inputs for the SD model calculations (hazardous models: flood hydrograph, earthquake, and initial state) provided in Figure 5(b).

The inputs and outputs from the SD model for five simulations are provided in Figure 6 and Table 4 only for illustrative purposes and present the several water system management solutions that the SD model could exercise. The inputs were randomly selected in order to respond to the water resources system under different severity of hazardous events. Considering the goals of this research, the illustrated outputs from the SD model highlight the variables related to flood protection facilities (e.g., water levels in the reservoir, spillway, and bottom outflows) required for the flood dynamic resilience quantification.
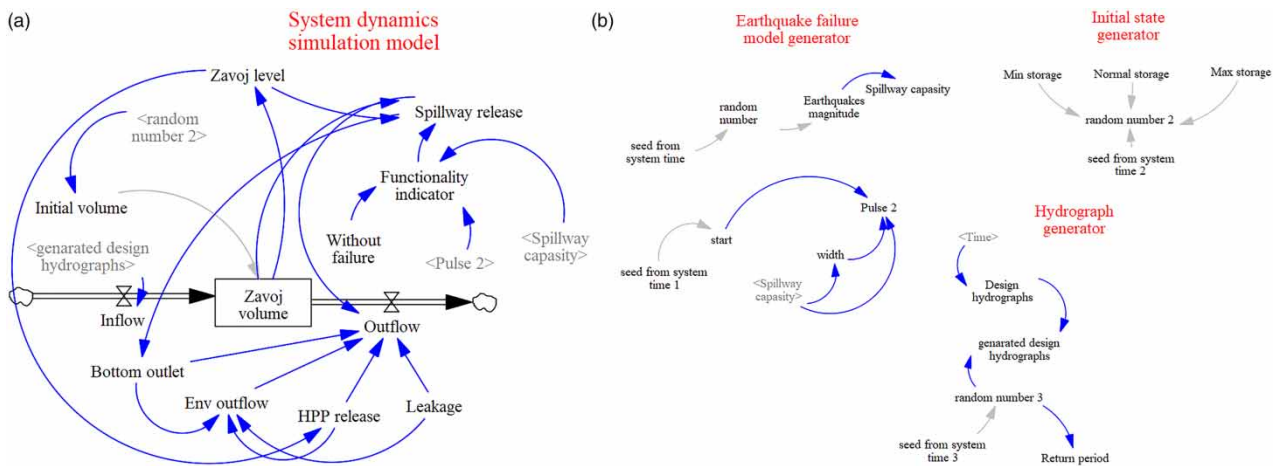
Figure 5 | System dynamics model of the Pirot water resources system (a) alongside hazardous models (b).

It can be seen from Figure 6 and Table 4 that the most severe flood event was generated in simulation 1. The hydrograph peak reached the value of 6,183 m³/s (Table 4), while the generated earthquake magnitude caused a relatively moderate decrease in the spillway functionality indicator (Figure 6(b)). The initial state in the reservoir, at the beginning of simulation 1, corresponds to the lowest water level respecting the result from all simulations (Figure 6(d) and 6(c)). Considering the generated inputs for simulation 1, especially in the terms of the extremely high flood hydrographs, the water levels in the Zavoj reservoir and spillway outflows reached the highest possible values (Figure 6(d) and 6(e)). Within this simulation, the bottom outflow had an important role since it assists in the discharging of the reservoir, alongside the spillway. Note that the total capacity of the bottom outflow (80 m³/s) is substantially lower than the spillway capacity (1,820 m³/s). Over the highest reached water level in the Zavoj reservoir, the bottom outflow facility released outflows up to its total capacity (Figure 6(e)).

For the case of simulation 4, the water levels in the Zavoj reservoir also achieved a maximal possible level. Such behavior of the Pirot corresponded to the highest value of the generated earthquake magnitude equal to 0.948 (Table 4), and consequently a hugely decreased capacity of the spillway (Figure 6(b)). However, a moderate peak of the generated hydrograph (Table 4) did not significantly affect the changes in the water reservoir levels.

The rest of the simulations (simulations 2, 3, and 5) produced a conservative system behavior since the increase of the water levels in the Zavoj reservoir was moderate (Figure 6(d)). This response of the Pirot water resources system is mainly attributed to the high capacity of the spillway (up to 1,820 m³/s) and corresponding values of spillway functionality indicators to discharge the reservoir during the flood events with the peaks in the range from 706 to 1,201 m³/s (Table 4). The most indicative are simulations 2 and 5 where the generated earthquake magnitudes did not cause any reduction of the spillway capacity, considering Equation (2). Therefore, the functionality indicators over the whole simulation time kept maximal values enabling the efficient transformation of flood hydrographs to downstream river sections (Figure 6(b)).

Flood dynamic resilience assessment

Flood dynamic resilience captures the Pirot water resources system capacity over simulation time to respond to and withstand hazardous events. The main properties of dynamic resilience are robustness and rapidity. Robustness is defined as the minimal value of dynamic resilience reached at the t_1 time step (Figure 2). The difference between the recovery time (t_1) and the time when a hazardous event occurs (t_0) is the system's rapidity.

A system performance level of the Pirot water resources system is defined by using Equation (8). When the water levels in the Zavoj reservoir are below the maximal operation levels, the system performance is equal to 1. By exceeding the predefined level, the performance level decreases to zero value. Following this, the flood dynamic resilience (Equation (7)) is quantified for each simulation time step with respect to the hazardous start time (t_0).

Examples of flood dynamic resilience quantification are shown in Figure 7. Using the outputs from the SD model (water levels) and predefined system performance level related to flood protection, the flood dynamic resilience was estimated for five simulations.
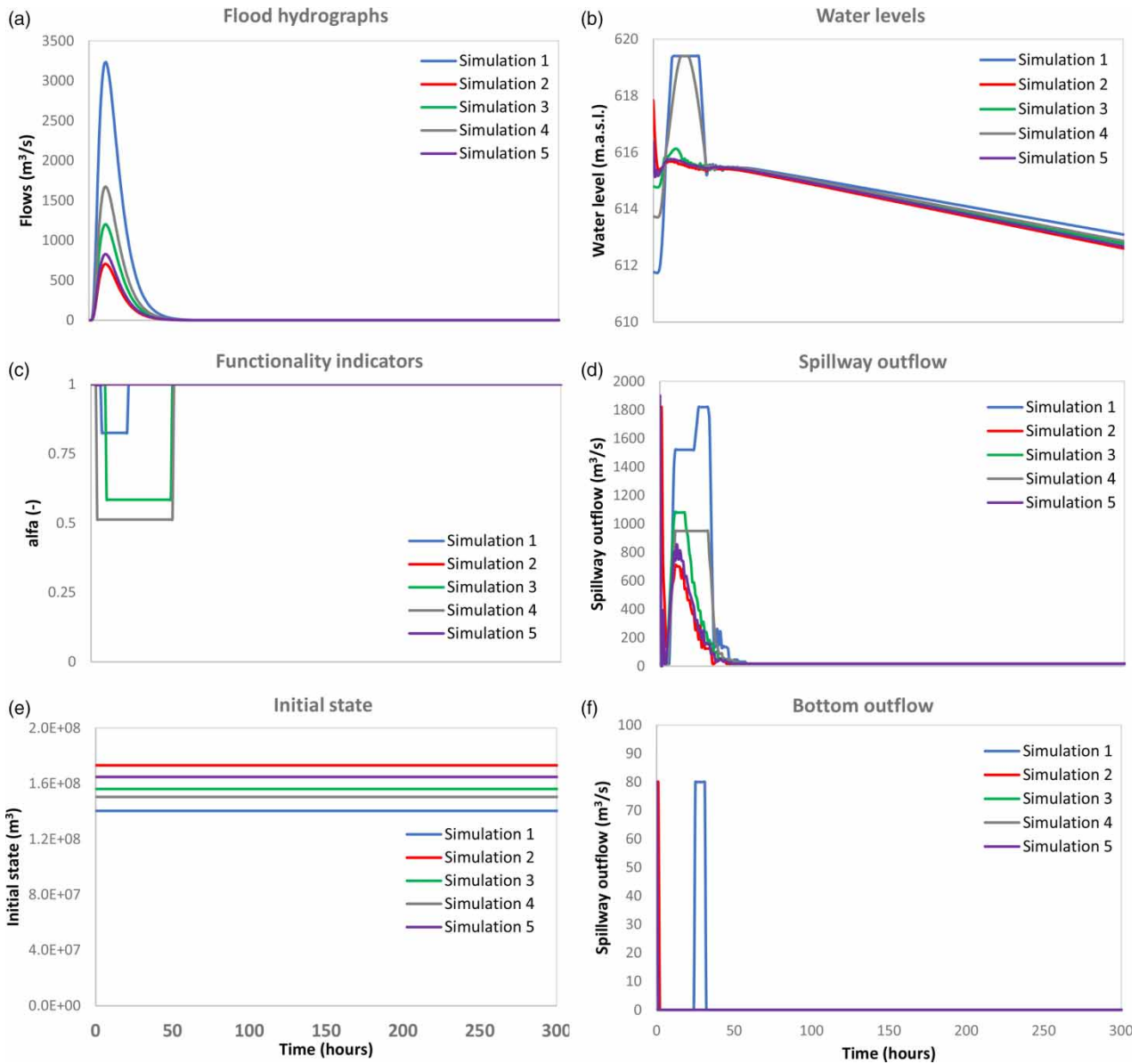
Figure 6 | Simulations of the SD model of the Pirot water resources system: inputs (a, b, c) and outputs (d, f, g).

Table 4 | Numerical values of the SD model simulations: T – return period, Q_{max} – maximal flood hydrograph value, a – standardized earthquake magnitude, $Q_{SW,max}$ – maximal spillway outflow, $Q_{BO,max}$ – bottom outflow, Z_{min} and Z_{max} – minimal and maximal water levels in the reservoir

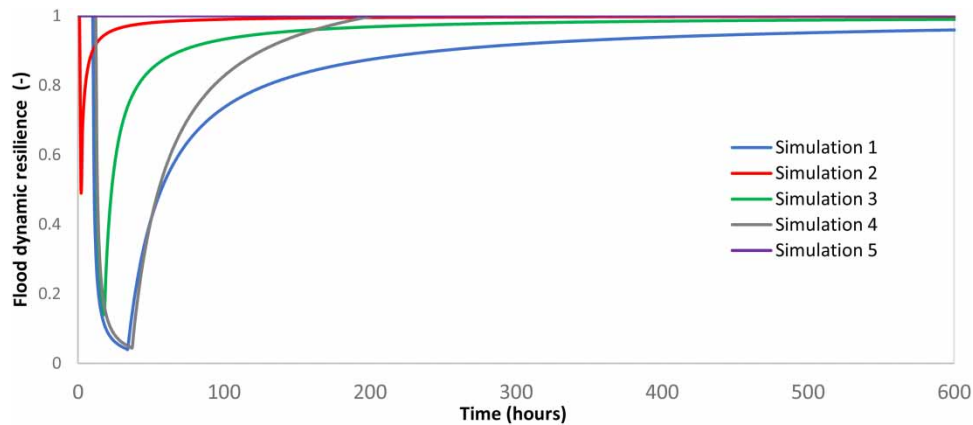| Simulation	T	Q_{max}	a	Z_{min}	Z_{max}	$Q_{SW,max}$	$Q_{BO,max}$
1	6,183	3,233	0.706	600.4	619.4	1,820	80
2	106	706	0.173	597.4	617.8	1,820	80
3	485	1,201	0.908	598.2	616.1	1,107	0
4	1,252	1,672	0.948	598.8	619.4	950	0
5	166	827	0.319	597.6	616.4	1,820	80

Figure 7 | Flood dynamic resilience quantification of the Pirot water resources system (from simulation 1 to simulation 5).

The results from Figure 7 suggest that the Pirot water system was less resilient (∼0.04) in the case of simulations 1 and 4. The former is attributed to the extraordinary values of the flood hydrograph resulting in the prolonged high water levels in the Zavoj reservoir. Although the latter is not characterized by the extremely high peak of the flood hydrograph, the reduced spillway capacity produced a low flood dynamic resilience. The important difference between these simulations lies in the fact that the dynamic resilience rapidly increased for simulation 4 since the duration of high-water levels was less when compared to simulation 1 (Figure 6(d)). Moreover, the Pirot water resources system implied a low resistance level for simulation 3 (0.143). For this simulation, the low flood resilience level is attributed to a substantial decrease in the spillway capacity (Table 4).

On the contrary, the most resilient system behavior was exhibited in simulation 5, maintaining the resilience value at the maximal level (Figure 7). Despite relatively high water levels at the beginning of the simulation (Figure 6(c)), the Pirot water resources system was not disturbed by significant hazardous events.

In the case of simulation 2, the high water levels in the Zavoj reservoir led to a rapid decrease of the flood dynamic resilience equal to 0.50 (Figure 7). Fortunately, the Pirot water resources system coped with the unfavorable starting conditions and promptly reached the full system performance (Figure 6(c)).

However, hazardous events from previous simulations may not provide a precise insight regarding the flood-related risks under hazardous events. To examine the system behavior in more detail, the total set of the generated data (1,000 simulations) were used to envelop hazardous events with low joint probability distributions. Such events are expected to lead to the water system operating out of the design envelopes and substantially increased flood-related risks. For the sake of a precise view of flood-related risk under hazardous events, flood dynamic resilience was researched in terms of robustness and rapidity by the use of a number of simulations (Figure 8). Please bear in mind that the simulations where potential hazards do not cause significant flood-related risks were singled out from the examined dataset and that only 1,000 simulations with flood dynamic resilience lower than 1 were considered.

For the most extreme hazard combination, the flood dynamic resilience decreased roughly to zero value. A decrease in robustness (with a minimum value of 0.03 given in Figure 8(a)) is brought about by combinations of earthquakes with significant magnitude and flood hydrographs with a low frequency of occurrence. To retrieve the system functionality under such severe hazards, the rapidity of the Pirot water resources system reached 1,000 h (Figure 8(c)). In the case of the moderate hazards, the system robustness had a median of 0.2 (Figure 8(a)) while rapidity was equal to 162 h (Figure 8(b)).

To examine the flood dynamic resilience in more detail, ANN was employed to model dependencies between hazardous events with different impacts on the system elements and flood-risk metrics (robustness and rapidity). For this purpose, a feed-forward neural network was used, with three input nodes, three hidden layers of four nodes each, and two output nodes. The network was fully connected, and the hidden, as well as the output layer activation functions, were all sigmoid. The network was trained using the LM algorithm (with 1,000 epochs). The ANN's inputs were: (1) the set of maximal values of generated flood hydrographs (Q_{max}); (2) the reduction of the functional indicators (α_{min}), and (3) the initial state (V_{start}) in the Zavoj reservoir. The dataset was split into three subsets: the training set, validation set, and test set using a 70%–15%–15% split, respectively. Additionally, the data for these subsets were selected randomly to preserve generality. The network was trained
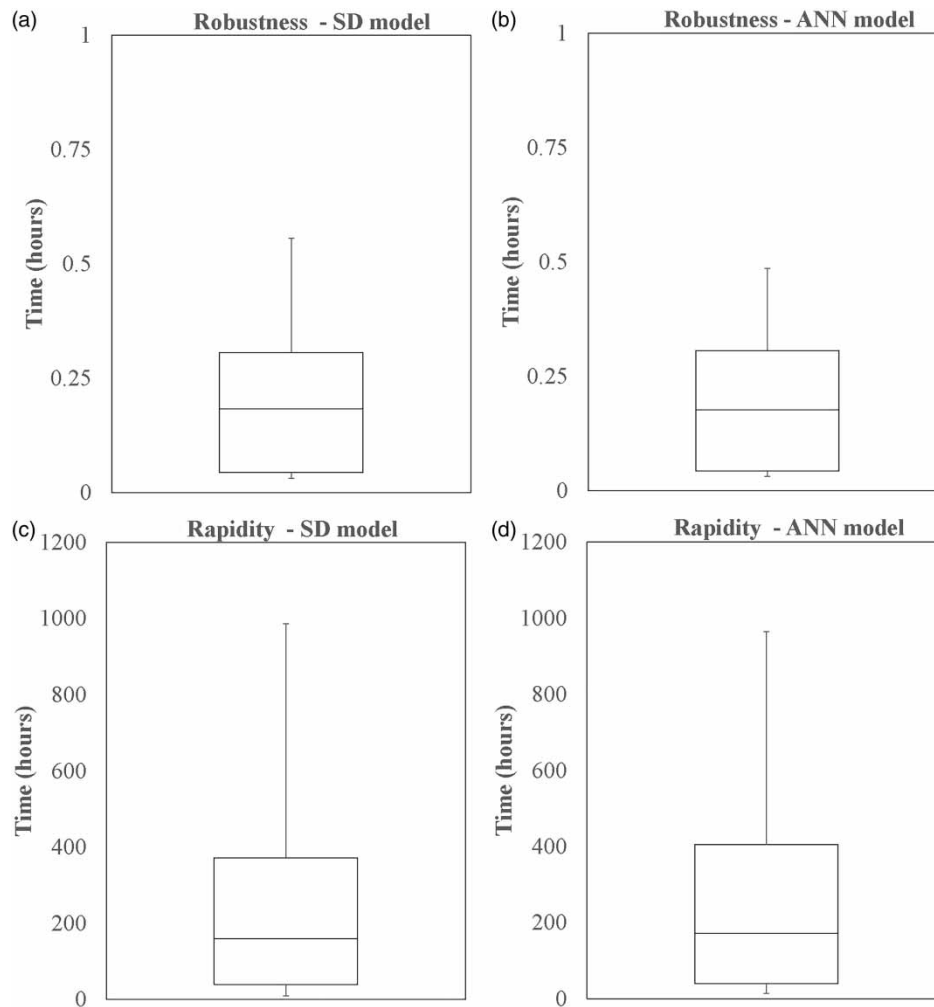
Figure 8 | Boxplots of flood dynamic resilience (Pirot water resources system) using the generated dataset: SD model – robustness (a); ANN model – robustness (b), SD model – rapidity (c), and SD model – rapidity (d).

200 times and the best of those networks was selected to avoid the problem of local minimum which can adversely affect the network's further application. The selection of the best network was based on the Root Mean Square Error (RMSE) metric. Note that when selecting the best network, robustness and rapidity were valued with equal importance.

The results imply that the ANN accurately reproduces key dynamic resilience parameters (Figure 8(b) and 8(d)) compared to their simulated values via the SD model (Figure 8(a) and 8(c)). For instance, the first and third quartiles on the boxplot diagrams expose similar values for both modeling approaches (SD and ANN models). However, slight discrepancies are indicated in the case of the second quartile (median) equal to $+3.3\%$ and -8.1% for robustness and rapidity, respectively (Figure 8). Maximal values of those parameters indicate that the ANN model slightly underestimates the extreme values derived by the SD approach (Figure 8).

The metric used to quantify the efficacy of the ANN approximation was the relative error; the average relative error was equal to 2.14% for robustness and 1.77% for rapidity. Moreover, the RMSE values for robustness and rapidity were equal to 0.004 (–) and 12.7 h, respectively. Considering the timespan of rapidity, such an error is not substantial.

The modeling errors for robustness and rapidity are shown in Figure 9 using the cumulative general extreme distributions since they fit the prolonged right distribution tails well.

Robustness and rapidity diverge from the corresponding observed parameters for higher values of cumulative distribution function (e.g., higher than 0.95), where robustness diverges more, the quantiles of the approximation distribution are more aligned with the observed parameters in the case of rapidity (Figure 9).
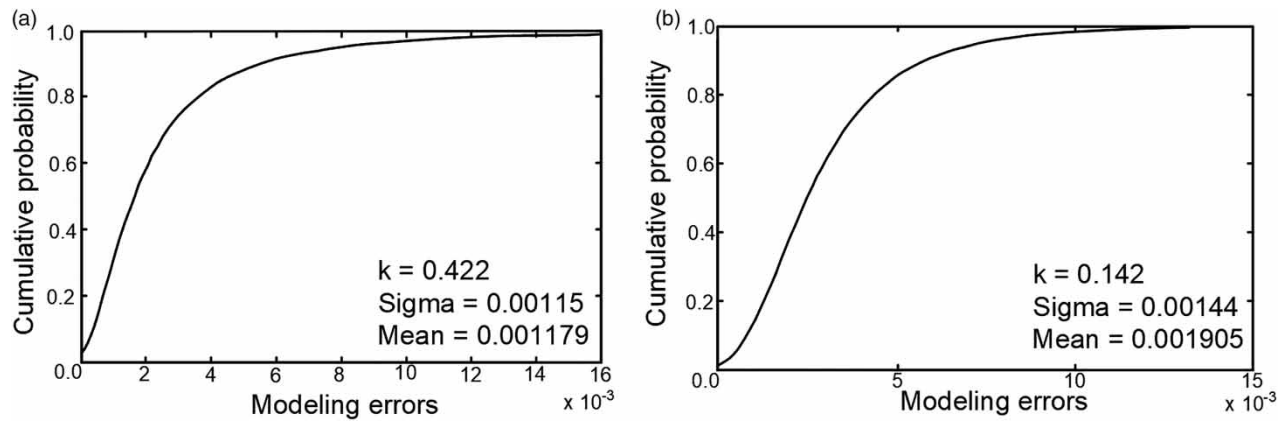
Figure 9 | Cumulative extreme value distribution function of the ANN modeling errors: (a) robustness and (b) rapidity.

However, the results (Figures 8 and 9) indicate that ANNs are capable of adequately approximating the wide range of the robustness and rapidity values needed for real-time operations of the Pirot water resources system. In addition, results indicate several accessible improvements: (1) simulations of the models are performed with the generated hydrographs instead of using a limited number of the observed flood events, (2) hazardous models envelop the most important system disturbances (floods and earthquakes) while other hazards and are not considered (e.g. failures of monitoring, electrical, or mechanical equipment), (3) sigmoid activation function may not catch the extremely high values of dynamic resilience-related parameters, and application of the ReLU activation function can improve prediction of the flood-related parameters (Bui et al. 2020).

DISCUSSION

Natural hazards encompass several physical phenomena such as floods, severe storms, earthquakes, landslides, and tornadoes (Gill & Malamud 2014). The southwest European region is sensitive to natural hazards since floods and earthquakes considerably exceeded the largest foreseen events and caused billions in damage (Stojković et al. 2017; Maršanić et al. 2021).

Therefore, this research is focused on the impacts of floods and earthquakes on the functionalities of the Pirot water system (located in Serbia, Southeast Europe) that prevent and reduce loss and damage due to extreme events. To examine the combination of a wide range of less and more severe hazards, we proposed a hazards modeling approach founded upon MC simulations that enable the simulation of hazardous events with low joint probability. Hazardous modeling reduces the uncertainty caused by short recording periods (Koutsoyiannis & Montanari 2007) using the stochastic weather generator creating long climate data (1,000 years span) needed for hydrological modeling (King et al. 2015). Hazardous modeling also encompasses the outputs from the Zavoj dam safety model to precisely deduce the dependence between the earthquake magnitude and functionality of the spillway (Rakić et al. 2022). In addition, MC simulations are used to derive variable water content in the water system since its initial condition significantly impacts on prevention of uncontrolled and rapid release from the system (Kistenmacher & Georgakakos 2015).

The behavior of the Pirot water resources system is simulated under a system dynamics approach enabling the system to respond to the generated hazardous events. A system approach deals with the difficulties introduced by the complexity of the water resources solutions and environmental issues (Simonovic 2020). It is especially highlighted when the system fails to execute the service requirements because of the reduced capacity of the flood-defense facilities under hazardous events. To measure the flood-related risk of the water system, dynamic resilience is used as a time-dependent parameter since it overperforms the static risks measures such as system reliability or vulnerability (Ignjatović et al. 2021). Based on the output from system dynamics simulations of the Pirot water system, the dynamic resilience captures the most important characteristics (Simonovic & Arunkumar 2016), specifically system robustness and rapidity (Figure 2). Rapidity describes the recovery time of the water resources system forced by an external or internal hazard (e.g., floods, failure of electrical or mechanical system facilities) (Bowles et al. 2013). A maximal reduced capacity of the water system in terms of delivering the service requirements is explained by robustness.

Considering an increase in available hydroclimatic data, alongside more computing power, machine learning algorithms become a useful method for flood risk and impact assessments (Wagenaar *et al.* 2020). In the presented research, flood-related risk characteristics (robustness and rapidity) were captured by postprocessing a huge amount of data generated via the system dynamics model. Then, the generated data, including the robustness and rapidity, was utilized for the supervised training of the ANN (Beale *et al.* 2020).

ANN was used to make a model for predicting robustness and rapidity based on characteristic values related to floods and earthquakes, and in the network training procedure, large data obtained from simulations of system dynamics models are used.

As mentioned before, the ANN was used to approximate flood-related risk characteristics, through the system modeling simulations. The results suggest that it is possible to train a network to approximate the rapidity and robustness of a system. Note that rapidity highly matches the target values since it continuously accumulates the flood-related risk characteristics over the simulation time. While the real system is more susceptible to measurement errors (e.g., measured water levels in reservoirs), the rapidity timescale allows for such errors to occur without significantly affecting resilience predictions. In contrast, the network cannot capture robustness with the same efficiency as rapidity because it changes rapidly after a disturbance is introduced.

There is an interest to consider the application of ANNs on a real system using actual data (Kostić *et al.* 2016; Allawi *et al.* 2018; Allawi *et al.* 2019; Jenny *et al.* 2020; Osman *et al.* 2020). However, its application is possible for the observed period with available records (inflows and water levels in the reservoir), while the usage of the developed system dynamics model cannot be avoided for predicational purposes where the inputs to the system and its behavior are unknown. Moreover, such an approximation is useful for managing water resources systems, as it can give an idea of when the system will return to a predisturbance level of functionality, helping operators to adequately allocate or reallocate resources to other systems, and improving overall functionality.

CONCLUSION

This paper proposes a novel framework for the evaluation of flood dynamic resilience for a water resources system under hazardous events, where the link between the hazardous events and the parameters used to evaluate flood dynamic resilience is defined by trained ANNs.

The proposed framework is tested on the Pirot water resources system located in Serbia. The framework is based on an SD modeling approach to mimic the non-linear behavior of the water resources system. The first of the hazardous models is a flood hydrograph model that is used to generate data sets using MC simulations based on uniform distribution. The second hazardous model is the earthquake model, which utilizes a functionality indicator (α) that is simulated using MC simulation in the range 0 to 1; this functionality indicator is derived from a simplified analytical form of ESWC values of the water resources system. The third hazardous model is the initial state model which uses a triangular distribution as input for MC simulations. Using the outputs from the SP modeling approach, flood dynamic resilience is estimated to capture several significant numerical characteristics (rapidity and robustness).

The framework relies on ANN which uses characteristic values of the hazardous models' outputs as inputs into the network to approximate flood dynamic resilience, exactly rapidity, and robustness. Quantifying the efficacy of the ANN approximation using the relative error metric shows an average relative error of 2.14% for robustness and 1.77% for rapidity. This is indicative of the fact that the ANN is properly trained. It is important to note that the robustness and rapidity diverge from the corresponding observed parameters for higher values of the cumulative distribution function; the robustness diverges more, while the quantiles of the approximated cumulative distribution are more aligned with the observed parameters in the case of rapidity. These diverging extreme values are to be expected given the sigmoid activation function, which may not catch the extreme values of flood dynamic resilience-related parameters. These results indicate that the ANNs are capable of adequately approximating the robustness and rapidity values caused by the hazards in the Pirot water resources system.

Future research may include several possible directions. For instance, the sigmoid activation function is used as an important part of the ANNs for flood dynamic resilience prediction. An improvement in the resilience prediction could be achieved by using the Rectified Linear Unit (ReLU) activation function instead of the sigmoid function. It helps to avoid the vanishing gradient phenomenon which can significantly hamper the learning progress (Goodfellow *et al.* 2016).

ACKNOWLEDGEMENTS

DATA AVAILABILITY STATEMENT

Data cannot be made publicly available; readers should contact the corresponding author for details.

CONFLICT OF INTEREST

The authors declare there is no conflict.

REFERENCES

Ahmad, S. & Simonovic, S. P. 2000 System dynamics modeling of reservoir operations for flood management. *Journal of Computing in Civil Engineering* **14** (3), 190–198.

Allawi, M. F., Jaafar, O., Mohamad Hamzah, F., Ehteram, M., Hossain, M. & El-Shafie, A. 2018 Operating a reservoir system based on the shark machine learning algorithm. *Environmental Earth Sciences* **77** (10), 1–14.

Allawi, M. F., Binti Othman, F., Afan, H. A., Ahmed, A. N., Hossain, M. S., Fai, C. M. & El-Shafie, A. 2019 Reservoir evaporation prediction modeling based on artificial intelligence methods. *Water* **11** (6), 1226.

Ardeshirtanha, K. & Sharafati, A. 2020 Assessment of water supply dam failure risk: development of new stochastic failure modes and effects analysis. *Water Resources Management* **34** (5), 1827–1841.

Assumma, V., Bottero, M., Datola, G., De Angelis, E. & Monaco, R. 2019 Dynamic models for exploring the resilience in territorial scenarios. *Sustainability* **12** (1), 3.

Beale, M. H., Hagan, M. T. & Demuth, H. B. 2020 *Deep Learning Toolbox: User's Guide (r2020a)*. The MathWorks, Inc, Natick, MA

Bocchiola, D. & Rosso, R. 2014 Safety of Italian dams in the face of flood hazard. *Advances in Water Resources* **71**, 23–31.

Bowles, D., Brown, A., Hughes, A., Morris, M., Sayers, P., Topple, A., Wallis, M. & Gardiner, K. 2013 *Environment Agency – Guide to Risk Assessment for Reservoir Safety Management, Volume 2: Methodology and Supporting Information Report – SC090001/R2*.

Bui, D. T., Hoang, N. D., Martínez-Álvarez, F., Ngo, P. T. T., Hoa, P. V., Pham, T. D., Samui, P. & Costache, R. 2020 A novel deep learning neural network approach for predicting flash flood susceptibility: a case study at a high frequency tropical storm area. *Science of The Total Environment* **701**, 134413.

Datola, G., Bottero, M., De Angelis, E. & Romagnoli, F. 2022 Operationalising resilience: a methodological framework for assessing urban resilience through system dynamics model. *Ecological Modelling* **465**, 109851.

De Angeli, S., Malamud, B. D., Rossi, L., Taylor, F. E., Trasforini, E. & Rudari, R. 2022 A multi-hazard framework for spatial-temporal impact analysis. *International Journal of Disaster Risk Reduction* **73**, 102829.

Environment Agency 2011 *Lessons From Historical Dam Incidents – Report SC080046/R1*.

Fan, X., Scaringi, G., Korup, O., West, A. J., van Westen, C. J., Tanyas, H., Hovius, N., Hales, T. C., Jibson, R. W., Allstadt, K. E. & Zhang, L. 2019 Earthquake-induced chains of geologic hazards: patterns, mechanisms, and impacts. *Reviews of Geophysics* **57** (2), 421–503.

Gill, J. C. & Malamud, B. D. 2014 Reviewing and visualizing the interactions of natural hazards. *Reviews of Geophysics* **52** (4), 680–722.

Gocić, M., Velimirovic, L., Stankovic, M. & Trajkovic, S. 2021 Regional precipitation-frequency analysis in Serbia based on methods of L-Moment. *Pure and Applied Geophysics* **178** (4), 1499–1511.

Goodfellow, I., Bengio, Y., Courville, A. & Bach, F. 2016 *Deep Learning (Adaptive Computation and Machine Learning Series)*. The MIT Press, Cambridge, MA, USA, p. 800.

Greco, R., Di Nardo, A. & Santonastaso, G. 2012 Resilience and entropy as indices of robustness of water distribution networks. *Journal of Hydroinformatics* **14** (3), 761–771.

Haktanir, T., Citakoglu, H. & Acanal, N. 2013 Fifteen-stage operation of gated spillways for flood routing management through artificial reservoirs. *Hydrological Sciences Journal* **58** (5), 1013–1031.

Hwang, H., Lansey, K. & Quintanar, D. R. 2015 Resilience-based failure mode effects and criticality analysis for regional water supply system. *Journal of Hydroinformatics* **17** (2), 193–210.

ICOLD, C. 2018 *Position Paper Dam Safety and Earthquakes*. Taylor & Francis Group, London.

Ignjatović, L., Stojković, M., Ivetić, D., Milašinović, M. & Milivojević, N. 2021 Quantifying multi-parameter dynamic resilience for complex reservoir systems using failure simulations: case study of the pirot reservoir system. *Water* **13** (22), 3157.

Jenny, H., Alonso, E. G., Wang, Y. & Minguez, R. 2020 *Using Artificial Intelligence for Smart Water Management Systems*.

Jiang, Y. & Zhang, Q. 2008 Design and Implementation of Dam Failure Risk Assessment System Based on Fuzzy Mathematics. In: *2008 IEEE International Symposium on Knowledge Acquisition and Modeling Workshop* (Wang, J., Zhao, C., Wu, Y. & Liu, Q., eds.). IEEE, New York, NY, pp. 486–489.

Kappes, M. S., Keiler, M., von Elverfeldt, K. & Glade, T. 2012 Challenges of analyzing multi-hazard risk: a review. *Natural Hazards* **64** (2), 1925–1958.

Karim, F., Hasan, M. & Marvanek, S. 2017 Evaluating annual maximum and partial duration series for estimating frequency of small magnitude floods. *Water* **9** (7), 481.

King, L. M. & Simonovic, S. P. 2020 A deterministic Monte Carlo simulation framework for dam safety flow control assessment. *Water* **12** (2), 505.

King, L. M., McLeod, A. I. & Simonovic, S. P. 2015 Improved weather generator algorithm for multisite simulation of precipitation and temperature. *JAWRA Journal of the American Water Resources Association* **51** (5), 1305–1320.

King, L. M., Schardong, A. & Simonovic, S. P. 2019 A combinatorial procedure to determine the full range of potential operating scenarios for a dam system. *Water Resources Management* **33** (4), 1451–1466.

Kistenmacher, M. & Georgakakos, A. P. 2015 Assessment of reservoir system variable forecasts. *Water Resources Research* **51** (5), 3437–3458.

Kostić, S., Stojković, M., Prohaska, S. & Vasović, N. 2016 Modeling of river flow rate as a function of rainfall and temperature using response surface methodology based on historical time series. *Journal of Hydroinformatics* **18** (4), 651–665.

Koutsoyiannis, D. & Montanari, A. 2007 Statistical analysis of hydroclimatic time series: uncertainty and insights. *Water Resources Research* **43**, 5.

Liang, Y., Wang, Y., Zhao, Y., Lu, Y. & Liu, X. 2019 Analysis and projection of flood hazards over China. *Water* **11** (5), 1022.

Major, J. 2019 *Bureau of Reclamation, Best Practices and Risk Methodology*. Basics of Probability and Statistics, online material. www.usbr.gov/ssle/damsafety/risk/methodology.html (accessed 1 March 2022).

Manfreda, S., Miglino, D. & Albertini, C. 2021 Impact of detention dams on the probability distribution of floods. *Hydrology and Earth System Sciences* **25** (7), 4231–4242.

Maršanić, V. B., Dobrović, N., Tadić, M. F. & Flander, G. B. 2021 2020 double crisis in Croatia: earthquakes in the time of COVID-19. *European Child & Adolescent Psychiatry* **30** (8), 1309–1313.

Men, B., Liu, H., Tian, W., Wu, Z. & Hui, J. 2019 The impact of reservoirs on runoff under climate change: a case of Nierji reservoir in China. *Water* **11** (5), 1005.

Nozari, H., Moradi, P. & Godarzi, E. 2021 Simulation and optimization of control system operation and surface water allocation based on system dynamics modeling. *Journal of Hydroinformatics* **23** (2), 211–230.

Osman, A., Afan, H. A., Allawi, M. F., Jaafar, O., Noureldin, A., Hamzah, F. M., Ahmed, A. N. & El-shafie, A. 2020 Adaptive Fast Orthogonal Search (FOS) algorithm for forecasting streamflow. *Journal of Hydrology* **586**, 124896.

Rakić, D., Stojković, M., Ivetić, D., Živković, M. & Milivojević, N. 2022 Failure assessment of embankment dam elements: case study of the Pirot reservoir system. *Applied Sciences* **12** (2), 558.

Simonovic, S. P. 2020 Application of the systems approach to the management of complex water systems. *Water* **12** (10), 2923.

Simonovic, S. P. 2021 Systems approach and performance-based water resources management. *Water International* **46** (7–8), 1224–1235.

Simonovic, S. P. & Arunkumar, R. 2016 Comparison of static and dynamic resilience for a multipurpose reservoir operation. *Water Resources Research* **52** (11), 8630–8649.

Stojkovic, M. & Simonovic, S. P. 2019 System dynamics approach for assessing the behaviour of the Lim Reservoir system (Serbia) under changing climate conditions. *Water* **11** (8), 1620.

Stojković, M., Prohaska, S. & Zlatanović, N. 2017 Estimation of flood frequencies from data sets with outliers using mixed distribution functions. *Journal of Applied Statistics* **44**, 2017–2035.

Tosun, H. 2015 *Earthquakes and Dams*. In Earthquake Engineering – From Engineering Seismology to Optimal Seismic Design of Engineering Structures. IntechOpen.

VenPy 2022 *Python Tools for Vensim*. https://github.com/pbreach/venpy (accessed 1 March 2022).

Vensim Reference Manual 2021 Available at: https://vensim.com/docs/ (accessed 1 March 2022).

Wagenaar, D., Curran, A., Balbi, M., Bhardwaj, A., Soden, R., Hartato, E., Mestav Sarica, G., Ruangpan, L., Molinario, G. & Lallemant, D. 2020 Invited perspectives: how machine learning will change flood risk and impact assessment. *Natural Hazards and Earth System Sciences* **20** (4), 1149–1161.

Xu, P., Wang, D., Singh, V. P., Lu, H., Wang, Y., Wu, J., Wang, L., Liu, J. & Zhang, J. 2020 Multivariate hazard assessment for nonstationary seasonal flood extremes considering climate change. *Journal of Geophysical Research: Atmospheres* **125** (18).

Yang, Z., Wang, Y., Yang, K., Hu, H., Song, S., Xu, S., Zhand, X., Ye, S. & Li, J. 2022 The energy, water supply, and ecology coordination for middle-long-term reservoirs scheduling with different connection modes using an elite mutation strategy-based NMOSFLA. *Journal of Hydroinformatics* **24** (6), 1091–1110.